Ground Water Monitoring&Remediation

Electrical Resistivity Imaging of a Permanganate Injection During In Situ Treatment of RDX-Contaminated Groundwater

by Todd Halihan, Jeffrey Albano, Steve D. Comfort, and Vitaly A. Zlotnik

Abstract

Groundwater beneath the former Nebraska Ordnance Plant (NOP) is contaminated with the explosive hexahydro-1,3,5-trinitro-1,3,5-triazine (RDX) and trichloroethene (TCE). Previous treatability experiments confirmed that permanganate could mineralize RDX in NOP aquifer material. The objective of this study was to determine the efficacy of permanganate to transform RDX in the field by monitoring a pilot-scale in situ chemical oxidation (ISCO) demonstration. In this demonstration, electrical resistivity imaging (ERI) was used to create two-dimensional (2-D) images of the test site prior to, during, and after injecting sodium permanganate. The ISCO was performed by using an extraction-injection well configuration to create a curtain of permanganate. Monitoring wells were positioned downgradient of the injection zone with the intent of capturing the permanganate-RDX plume. Differencing between ERI taken preinjection and postinjection determined the initial distribution of the injected permanganate. ERI also quantitatively corroborated the hydraulic conductivity distribution across the site. Groundwater samples from 12 downgradient wells and 8 direct-push profiles did not provide enough data to quantify the distribution and flow of the injected permanganate. ERI, however, showed that the permanganate injection flowed against the regional groundwater gradient and migrated below monitoring well screens. ERI combined with monitoring well samples helped explain the permanganate dynamics in downgradient wells and support the use of ERI as a means of monitoring ISCO injections.

Introduction

The former Nebraska Ordnance Plant (NOP) was a military loading and packing facility that produced bombs, boosters, and shells during World War II and the Korean War. During ordnance production, wastewater was routinely discharged into unlined ditches, resulting in severe soil and groundwater contamination. An estimated 23 billion gallons of water under approximately 6000 acres are contaminated with hexahydro-1,3,5-trinitro-1,3,5-triazine (RDX) and trichloroethene (TCE), or both at concentrations above health advisory levels (2 RDX μg/L) or maximum contaminant levels (5 TCE μg/L). To prevent the contaminated plume from migrating off-site and in the direction of municipal well fields, an elaborate series of extraction wells and piping networks were constructed to hydraulically contain the leading edge of the RDX/TCE plume. This extracted groundwater is currently pumped to a $33 million dollar treatment facility where approximately 4 million gallons of groundwater are filtered through granular activated carbon (GAC) each day. Recent estimates indicate that this pump and treat facility will need to operate in excess of 125 years to effectively manage the RDX/TCE plume (Comfort 2005).

Past work by Adam et al. (2004) showed that permanganate could effectively mineralize RDX in the presence of aquifer solids. Using sediments and groundwater from the NOP, Albano (2009) performed treatability experiments and confirmed that site conditions at NOP were conducive to using permanganate as an ISCO treatment. The first objective of this study was to determine the efficacy of permanganate to transform RDX at the field scale by performing a pilot-scale in situ chemical oxidation (ISCO) demonstration (Albano et al. 2010). Assessing the effectiveness of ISCO treatments typically involves discrete point sampling using wells or multilevel piezometers along anticipated flowpaths. Small variations in hydraulic conductivity, however, can divert groundwater flow away from anticipated flowpaths, frustrating efforts to monitor remediation efforts with preplaced wells. Without a dense network of multilevel piezometers throughout the area of interest, point sampling cannot reliably determine the spatial distribution of contaminant or

doi: 10.1111/j1745–6592.2011.01361.x

the flow of the injectate. An alternative to multiple-point sampling is to use the geophysical technique of electrical resistivity imaging (ERI). ERI uses arrays of easily placed, minimally invasive electrodes to measure apparent electrical resistivity from the surface. The technique requires a correlation between the groundwater solute concentration and the bulk electrical resistivity of the subsurface.

Electrical resistivity monitoring of injections is traditionally performed with subsurface electrodes (Ramirez et al. 1993; Daily et al. 2004). These experiments can significantly enhance quantitative characterization of subsurface properties (Singha and Gorelick 2006a, 2006b), but have limited spatial coverage and high costs. Surface monitoring using ERI is much more flexible and cost effective, but additional knowledge may be needed a priori, for a particular site or contaminant. A surface ERI monitoring effort was performed on a site in Ohio to evaluate ISCO treatment of TCE with permanganate (Nyquist et al. 1999). Results provided proof-of-concept for using ERI to map permanganate distribution but also identified the difficulty applying ERI a priori to complicated subsurface conditions.

For this study, ERI technology was utilized in an attempt to quantify the distribution of the permanganate following injection and to potentially record groundwater reactions that generated resistivity changes in the subsurface. Given that permanganate concentrations used for remediation purposes can have resistivities much lower than the ambient groundwater values, it was believed that this difference should be great enough to be measured by ERI (a factor of 28 times more conductive for this site, with a background fluid of 0.363 mS/cm and an injectate conductivity of 10.2 mS/cm). Likewise, the field site was the subject of an intensive previous investigation (Wani et al. 2007), so the site was deemed to be a "well characterized" porous media aquifer with sufficient well network to observe the injection.

Methods and Materials

Geology of Permanganate Injection Site

The geology at the permanganate injection site (N 41° 9' 24", W 96° 27' 117") is known from previous investigations by Woodward-Clyde (1995). Cross sections based on borehole logs show approximately 6.1 m (20 feet) of Peoria Loess mantling the Todd Valley Formation, which is comprised of approximately 15.2 m (50 feet) of fine sand and approximately 13.7 m (45 feet) of coarse sand.

Soil cores were collected using a Macro-Core setup with a direct-push GeoProbe® Model 6610DT, and borehole electrical conductivity was measured every 0.015 m (0.05 feet) using a Geoprobe® Direct Image Electrical Conductivity System. These data were converted to electrical resistivity (Ωm). Maximum core depth was 22.3 m (75 feet) below ground surface (bgs). Cores were analyzed for grain-size distribution. Interpretations of direct-push conductivity data were interpreted using core data, well logs, and cross sections from the previous work at the site (Woodward-Clyde 1995).

Aquifer Characterization

Permanganate transport in the subsurface is controlled by aquifer heterogeneity in hydraulic conductivity (Seol et al. 2003). To quantify aquifer heterogeneities within the injection site, full-screen pneumatic slug tests (Zurbuchen et al. 2002) were conducted on 12 existing wells installed by Wani et al. (2007), and in 6 additional monitoring wells that were added for this study (Figure 1). All wells at the site are screened in the upper fine sand layer of the Todd Valley aquifer 16.7 to 22.9 m (55 to 75 feet) bgs. Slug test results showed that values of horizontal hydraulic conductivity (K_h) ranged from 4 to 20 m/d (13 to 66 ft/d). In addition to full-screen pneumatic slug tests, multilevel

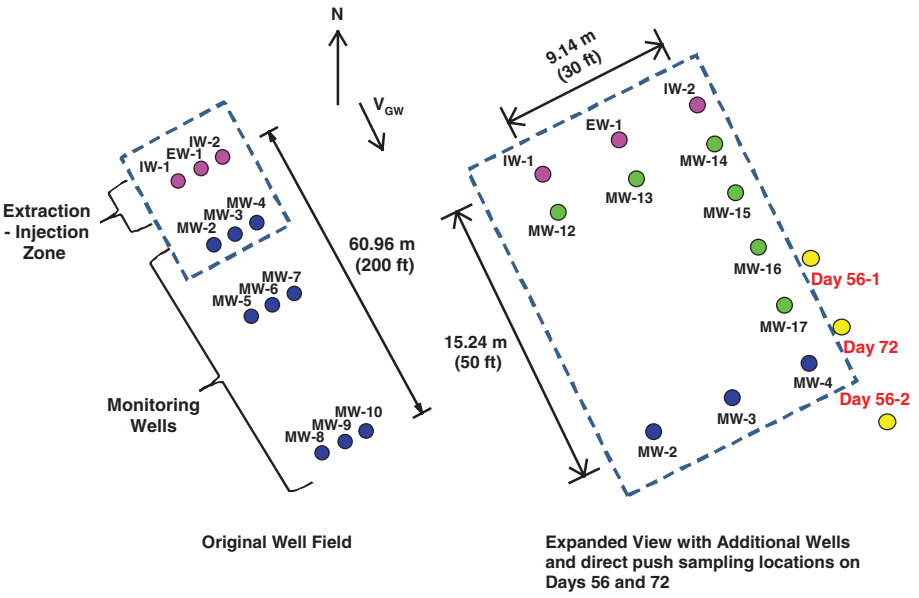

Figure 1. Extraction-injection wells and monitoring well network (left) with expanded view displaying additional wells added for this study and locations of direct-push sampling of groundwater.

pneumatic slug tests (Zlotnik and McGuire 1998; Zlotnik and Zurbachen 2003) were performed on a 10-cm monitoring well within the study site (MW-15) to quantify vertical variations in K_h along the well screen. The multilevel slug test data collected in MW-15 yielded K_h ranging from 3 to 27 m/d with highest conductive intervals between 18.9 m (62 feet) and 19.8 m (65 feet) bgs (Albano et al. 2010).

Permanganate Extraction–Injection Procedure

An extraction-injection procedure was used to deliver the permanganate to the groundwater in an attempt to create a curtain of permanganate between injection wells. Sodium permanganate ($NaMnO_4$) was injected into the groundwater via a proportional mixing-injection trailer system (Aquifer Solutions Inc., Evergreen, CO, USA). Groundwater was extracted from a center extraction well (EW-1) (Figure 1) via a submersible pump (Aermotor A+ 75-500, Delavan, WI, USA) at a rate of 151.6 L/min (40 gpm) and delivered to an intake manifold located onboard the trailer system. Approximately 1707 L (451 gallons) of 40% (w/w) $NaMnO_4$, was pumped at 3.8 L/min (1 gpm) from 1040 L (275 gallons) totes to the intake manifold where extracted groundwater and $NaMnO_4$ were mixed at a ratio of 40:1 for a total injectate volume of approximately 68,000 L (Halihan et al. 2009). The solution was gravity fed into two neighboring injection wells, IW-1 and IW-2 (Figure 1), at approximately 77.7 L/min (20.5 gpm). $NaMnO_4$ was continuously injected for 413 min. Following the injection, extracted groundwater from EW-1 was recirculated to wells IW-1 and IW-2 for 42 min.

During the injection, MnO_4^- concentrations were periodically measured on-site with a portable spectrophotometer (Hach model DR 2800, Loveland, CO, USA) to monitor permanganate concentration delivered to the injection wells and breakthrough at the extraction well. Specific conductivity was measured using a YSI 3000 T-L-C meter (Yellow Springs, OH, USA) during each MnO_4^- measurement to establish a calibration curve, similar to that used by Cavé et al. (2007) to relate specific conductivity to MnO_4^- concentration.

ERI of Permanganate Injection

ERI data were collected 1 month before; during; and 1, 30, 60, and 90 d following the injection. Electrodes were deployed along lines running parallel and perpendicular to the local groundwater gradient, using a line of 56 electrodes. Stainless steel stakes were inserted about 15 cm (0.5 feet) into the ground and connected to a *SuperSting R8* (Advanced Geosciences Inc., Austin, TX) system that executed a program to induce currents, measure potentials, and store the data. Electrode spacing determines the horizontal and vertical extent, and the spatial resolution of the measurements. Three-meter spacing was used for all ERI data collection except for 6-m spacing used on lines 6, D, E, and G, 90 d postinjection (Figure 2). Data were processed using a proprietary Halihan/Fenstemaker technique (Halihan and Fenstemaker 2004) to create two-dimensional (2-D) vertical models, or pseudosections, of the distribution of electrical resistivity. Three-meter spacing produces

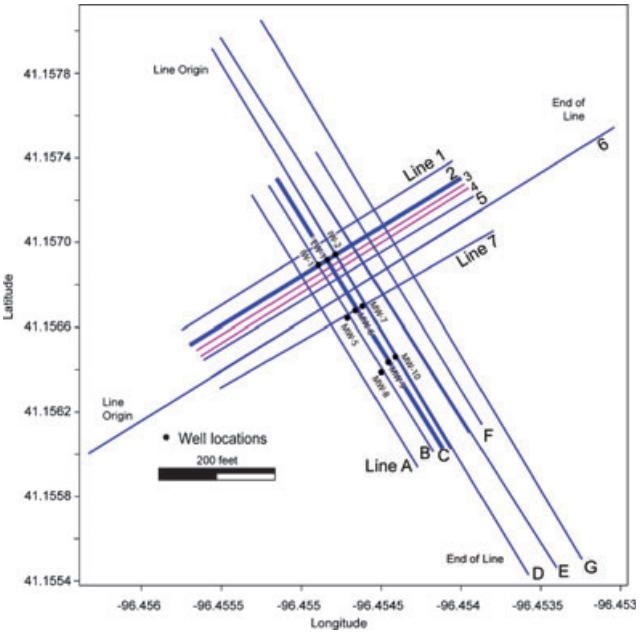

Figure 2. Map of 12 primary ERI line locations and monitoring wells for the site. Heavy blue ERI lines C and 2 were used as monitoring ERI lines during injection. Purple ERI lines 3 and 4, and extensions of lines 6, D, E, and G were not collected prior to injection.

pseudosections 165-m (541 feet) long and 33-m (108 feet) deep with a horizontal and vertical resolution of 1.5 m (4.9 feet); 6-m spacing produces a pseudosection 330-m (1082 feet) long and 66-m (216 feet) deep with a resolution of 3 m (9.8 feet). Pseudosections are presented as images colored to represent the distribution of modeled electrical resistivity. Figure 3 shows pseudosections along the same line (line D), collected with 3-m (Figure 3A) and 6-m (Figure 3B) spacing. The 3-m electrode spacing was selected to vertically center the extraction and injection well screens within the model domain. Data were collected with 6-m spacing in attempt to track injectate migration and evaluate the resistivity properties below the well field.

Background data collected one month prior to the injection were collected along lines 1, 2, 5 through 7, and A through E (Figure 2). During and immediately following the permanganate injection, ERI data were collected along 12 lines at the site. Lines 2 and C were collected before and during injection without moving the ERI setup for the highest level of precision in differencing the datasets. ERI data collected at later dates (i.e., 30, 60, 90 d postinjection) were not useful in tracking the injectate as electrodes were not left in situ at the site during the experiment, and the injectate had migrated deeper than expected.

Groundwater Sampling

Groundwater samples were collected from monitoring wells twice each week for 8 weeks following the injection. On each occasion, prior to sampling, specific electrical conductivity was measured using a YSI 3000 T-L-C meter at 0.6-m (2 feet) intervals in each well. Permanganate injectate concentrations were calculated using these specific

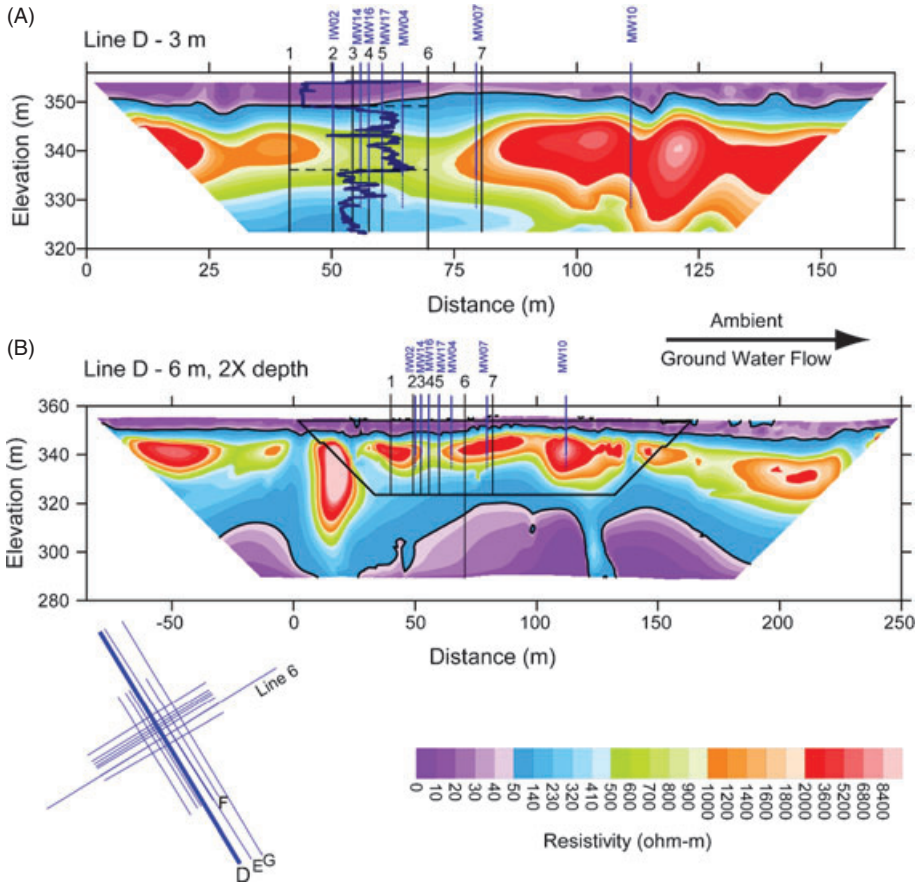

Figure 3. 2-D ERI pseudosections of ERI line D (map at lower left indicates setting relative to other lines). Blue lines indicate location of monitoring wells. Black lines show where perpendicular ERI lines (lines 1 to 7) intersect line D. Horizontal axes both have origins at the zero of the 3-m pseudosection. Injection plane is located at 50 m. (A) A 3-m spacing ERI image (165 m total length). Direct-push resistivity log overlaid on image along with black dashed lines indicating formation boundaries. (B) A 6-m electrode spacing ERI image (330 m total length). Black trapezoid indicates the spatial extent of the line shown in Figure 5.

conductivity measurements and the calibration curve created during the injection. Groundwater was then withdrawn from wells using a Grundfos Redi-flo2 submersible environmental pump (Olathe, KS, USA) and variable frequency drive converter. A minimum of three well volumes were withdrawn before taking two samples from each well, one for RDX and the other for MnO_4^-.

Groundwater samples were obtained at discrete 1.2-m intervals using direct-push technology (Geoprobe® Model 6610DT) with sampling points guided by ERI data (Figure 1). A groundwater sampling assembly of an outer casing and a subassembly of a steel rod, well screen, and drive point was driven to depths of 29 to 31 m bgs (95 to 102 feet), deeper than the bottom of monitoring well screens which were located at approximately 23 m (75 feet). At the target depth, the assembly was filled from the top with water to compensate for stress developed by penetrated overburden, and the outer casing was lifted to expose the screen. An inertial pump was used to withdraw three well volumes of water, followed by a sample. Once a sample had been collected, the rod assembly was raised approximately 1.22 m (4 feet), and the sampling cycle was repeated. Sampling continued until the screen reached the water table.

Results

Background ERI

Background 2-D inversion model results (pseudosections) created from ERI data collected 1 month prior to the injection and taken parallel to each other showed geologically consistent patterns. Perpendicular pseudosections also matched reasonably well. The relatively low resistivity of the upper horizon of the site was an initial concern with regard to imaging the injection, but at the expected resistivities and distribution of the injectate, it was not expected to pose a significant problem. What was unexpected was the significant variability in resistivity in the aquifer at the injection zone.

ERI pseudosections of the test plot prior to permanganate injection indicated a shallow low-resistivity layer (less than 100 Ωm) that extended between 4 and 5 m (13 to 16 feet) to an elevation of approximately 350 m (1150 feet; Figure 3). Beneath that layer was a highly variable layer that extended 20 to 30 m (66 to 98 feet) deep with a range in resistivity from 100 to 10,000 Ωm. This variable layer ended at an elevation of approximately 320 m (1050 feet) in the 3-m image domain, but the 6-m datasets indicate

that this layer extends to lower elevation at other locations (Figure 3). The pseudosection created from data collected along the same line, but with 6-m spacing and about 90 d postinjection, shows an irregular pattern of low to very low resistivity extending to the bottom of the pseudosection at about 290 m (950 feet) elevation (Figure 3B).

The direct-push electrical resistivity log was overlain and compared with ERI pseudosections (Figure 3A). Direct-push resistivity and surface ERI value patterns match exceptionally well for large features, showing a very conductive soil at the surface to a depth of about 5 m (16.4 feet), underlain by about 16 m (52 feet) of more resistive material, underlain in turn by a somewhat less resistive unit. These distributions correlate well with material observed in the extracted core and with the cross sections of Woodward-Clyde (1995). However, the higher resolution direct-push log identified, for example, a silty sand lens at a depth of about 10 m (33 feet) that was too thin for surficial ERI measurements to distinguish. The upper low-resistivity layer corresponds well to the thickness and expected resistivity of the Peoria Loess; the subordinate higher resistivity unit corresponds with the upper fine sand of the Todd Valley Formation; and the lower resistivities at the bottom of the direct-push log correspond with the lower coarse sand. The ERI pseudosections and the sediment logging from previous work agree again on the location of the Dakota Group, which appears to occur at an elevation of approximately 320 m (1050 feet) above sea level on a NAD27 datum (Figure 3) (Woodward-Clyde 1995).

Further, ERI model values were compared with hydraulic conductivity (K_h) data collected for the entire monitoring well system at the site (Figure 4). A significant increasing trend exists between the geometric mean ERI values for the screened intervals of the monitoring wells (16.7 to 22.9 m, 55 to 75 feet) and the hydraulic conductivity determined by full-screen pneumatic slug tests (Albano et al. 2010). Although a simple logarithmic trend exists over the range of the existing slug test data, the ERI transient injection results (discussed below) as well as the hydraulic conductivity data indicate that when resistivity values are greater than 5000 Ωm, hydraulic conductivity decreases. The lower hydraulic conductivity resulted from either compaction or cementation and that higher ERI values reflect lower porosity in this material (Albano et al. 2010). This is also supported by the circumstantial evidence obtained during direct-push sampling where high resistivity zones were extremely difficult to penetrate.

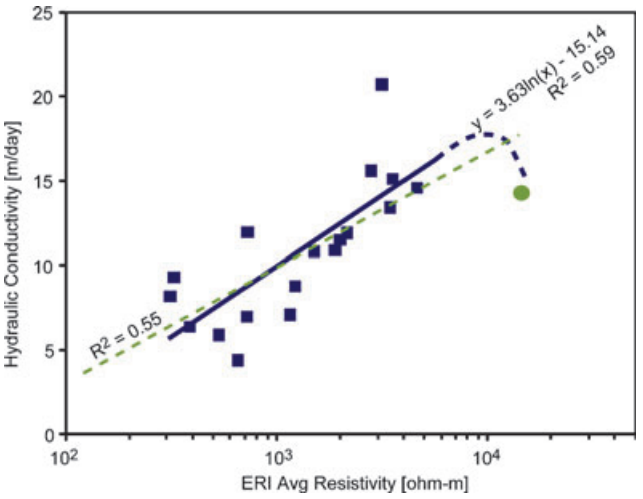

Figure 4. Geometric average of ERI model resistivity for location of screened intervals of monitoring wells compared with the hydraulic conductivity at the wells. The trend (solid blue line) indicates a general increase in hydraulic conductivity with increases in resistivity omitting the value of the green point. The dashed portion of the blue line indicates the expected trend when factoring in the results of the injection test which supported a conclusion that the high resistivity areas (greater than ~5000 Ωm) were less hydraulically conductive. Dash green line indicates fit if the green high resistivity point is included in the analysis.

Injection Monitoring by ERI

On the basis of previous reports (Wani et al. 2007), the injectate was expected to generate a "curtain" of permanganate that moved through the well field over several weeks. The volume and conductivity of the injectate was expected to cause significant changes to the resistivity images in the zone of the well screens. ERI pseudosections, however, showed no large changes in resistivity postinjection. Aside from the unexpected movement of the injectate (explained below), two properties appeared to have affected the ERI analysis: the subsurface material distribution and the fluid distribution. The site can electrically be approximated as a two-layer system. The upper layer resistivities were on the order of 10 Ωm (lower than expected) while the aquifer was on the order of 1000 Ωm (higher than expected). This yields a ratio of approximately 100 between the two layers. The upper, electrically conductive layer of silt suppressed the ER signal because of the large contrast with the aquifer material. Additionally, the ratio of the upper layer thickness (~6 m) to the electrode spacing (3 m) was only 0.5, which makes interpretation more difficult because of limited sensitivity (Telford et al. 1990).

Although the test site provided a challenging stratigraphy that limited quantitative assessment of the injection, arithmetic differencing between preinjection and postinjection ERI models revealed some discernable changes that allowed us to determine the distribution of the permanganate following injection. The majority of these changes were observed on the lines B and D, and transects where the stakes were not moved between surveys (lines 2 and C, Figures 5 and 6). Along these transects, both increases and decreases in resistivity occurred. The changes ranged from −13% to 13% (100× (later − earlier) / earlier), which were smaller than expected. The pseudosections show that significant changes occurred above the water table. Other changes occurred upgradient of the injection wells and vertically below and to the southwest of the injection wells. These changes were consistent with a conductive injectate being placed in the aquifer. The changes occurred over the entire injection curtain zone between IW-01 and IW-02. Pseudosections show increased resistivity beneath a road that crosses the site (Figure 6) and some areas near the water table, which may indicate areas that drained by the pumping at EW-01 during the injection phase.

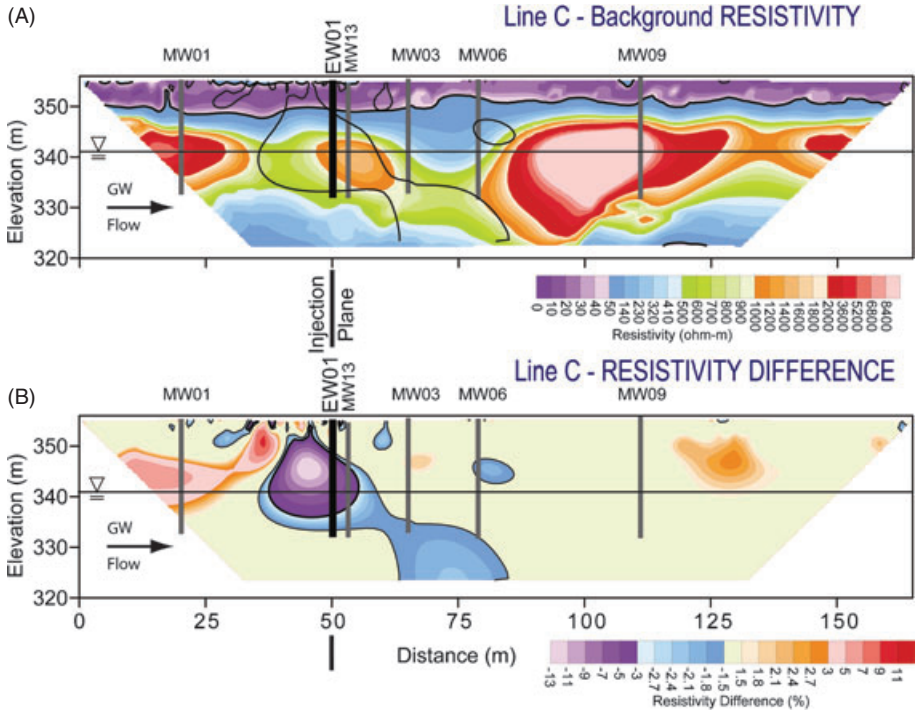

Figure 5. ERI data from line C (parallel to natural gradient direction). Black horizontal line indicates the location of the water table. Dark gray vertical lines indicate the locations of monitoring wells. Dark black vertical line indicates the location of the injection plane and injection well EW01. (A) Resistivity of ERI line C. Overlay indicates area of decreasing resistivity after injection superimposed on ERI image before injection. (B) Resistivity difference before and after injection.

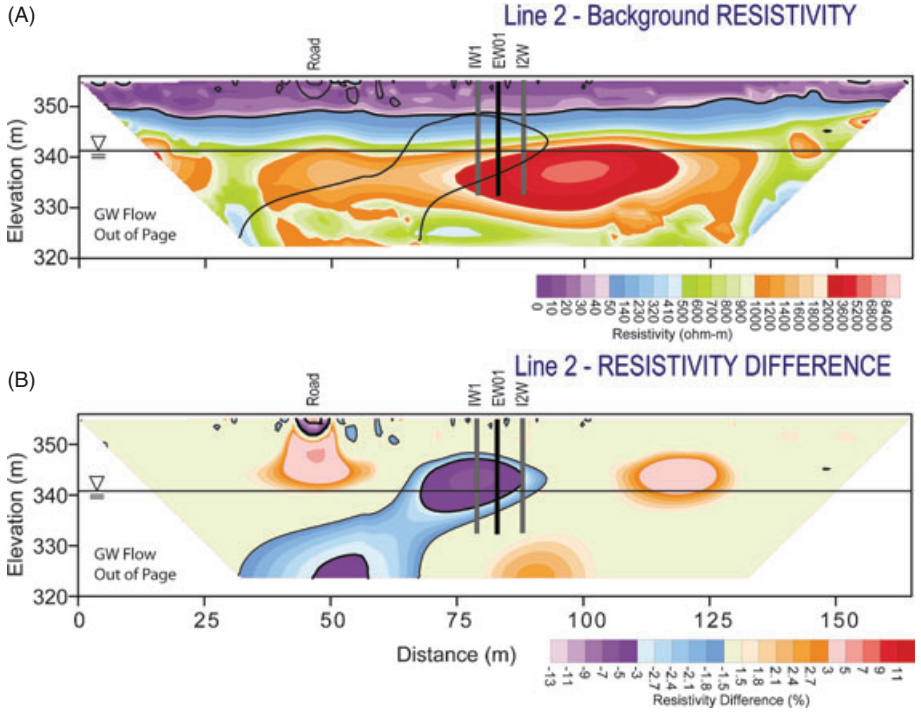

Figure 6. ERI data from line 2 (in injection plane, orthogonal to natural gradient). Black horizontal line indicates the location of the water table. Dark gray vertical lines indicate the locations of extraction wells. Dark black vertical line indicates the location of the injection well EW01. (A) Resistivity of ERI line 2. Overlay indicates area of decreasing resistivity after injection superimposed on ERI image before injection. (B) Resistivity difference before and after injection.

The areas where model differencing showed decreased resistivity were superimposed on preinjection images and corresponded with the higher hydraulic conductivity areas mapped by ERI (Figures 5A and 6A). Areas showing decreased resistivity were associated with the medium resistivity region (green) and the region under the high resistivity area at 100 m on line C (red to pink region of Figure 5A). Likewise, injectate under line 2 appeared to

avoid the highly resistive zone (red) at 100 m lateral distance (Figure 6).

On the basis of the extraction-injection well configuration (Albano 2009), and our model that assumed piston-type flow (i.e., no dispersion), approximately 7 h (420 min) of pumping (extraction-injection) would have been needed to complete the permanganate curtain (Albano et al. 2010). Initial permanganate breakthrough at the extraction well, however, was observed within 77 min (more than five times faster than expected). Once all the permanganate had been injected into IW-1 and IW-2 (t ~ 7.15 h), the permanganate concentration in EW-1 had only reached 2386 mg/L (vs. 15,300 mg/L injected), indicating that a uniform curtain of permanganate was not established across the injection wells. ERI results from differencing of lines B, C and D further supported this observation (Figure 7). Line C, which was directly over the extraction well, had the smallest change in resistivity. Lines over the injection wells had changes approximately twice the value of changes in the line over the extraction well (Figure 7). This further indicates that a permanganate curtain was not adequately established between the two injection wells.

Temporal Changes in Injectate

Permanganate breakthrough was observed in all wells within the field site except MW-2 and MW-3. Electrical conductivity measurements conducted in the monitoring wells prior to groundwater sampling revealed spatial differences in how the permanganate plume was entering the well screen. Results showed that the permanganate did not uniformly enter the monitoring well screens. The vertical variation indicates that the injectate followed the preferential flowpaths similar to those found during multilevel slug testing of MW-15 prior to permanganate injection (Albano et al. 2010). Calculated hydraulic conductivities (K_h) for MW-15 range from 3 to 27 m/d with the most conductive intervals between 18.9 and 19.8 m bgs. Assuming that this pattern occurs throughout the aquifer, samples withdrawn from monitoring wells comprise mixtures of waters affected and unaffected by the injectate. Thus, samples from monitoring wells show lower values of permanganate and higher values of RDX than aquifer volumes affected by the injectate (Albano et al. 2010).

Groundwater sampling conducted via direct push (DPT) at 56 and 72 d also showed permanganate plume bifurcation or plume fingering within the site. This bifurcation may be due to preferential pathways within the Todd Valley sands, deposited in a braided stream system similar to the current Platte River, which runs near the test site. The sedimentology of a braided stream is complex, with several channels, high width/depth ratios, steep slopes, and low sinuosities (Miall 1977).

Results from DPT sampling verified that permanganate migrated below the well screens of the monitoring wells (22.9 m, 75 feet) (Table 1). DPT sampling showed a direct relationship between the depths at which high permanganate and low RDX concentrations were observed. This was particularly evident on Day 56 where many of the depths that had no detected permanganate concentrations also had no detectable RDX (Table 1). Conversely, when permanganate was detected, so was RDX. Given that the kinetics of the permanganate-RDX reaction is much slower than that observed with chlorinated ethenes (Chokejaroenrat et al. 2011), it is not surprising that both permanganate and RDX were found together. This further indicates that the injected permanganate followed preferential pathways that were also transporting the highly mobile (low adsorbing) RDX. Direct-push sampling also revealed that the permanganate was moving as fingers less than 1.2 m (4 feet) thick. Given that the resolution of the ERI technique as performed was

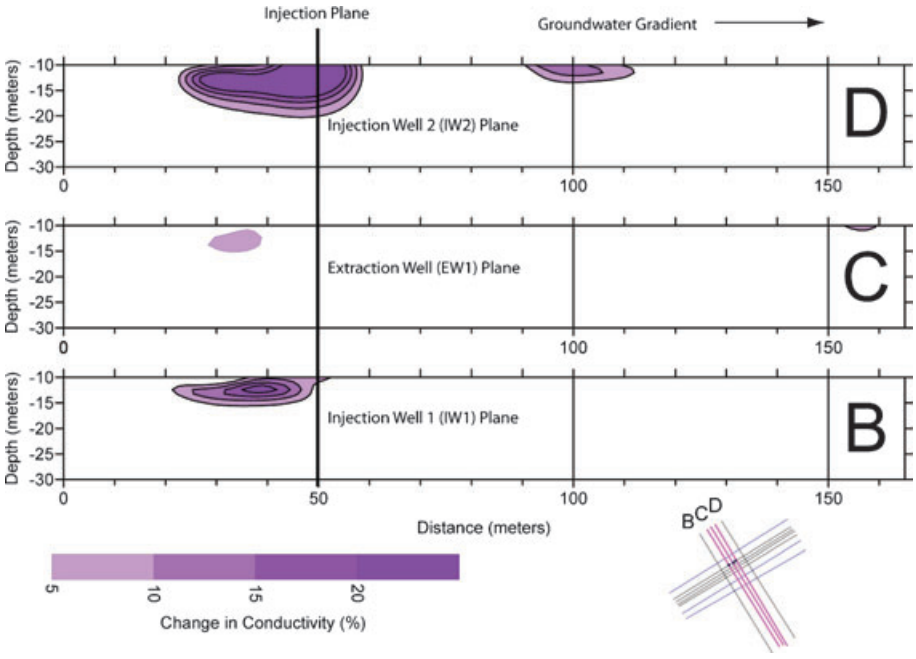

Figure 7. ERI differences along ERI lines B, C, and D. Data collected for lines B and D by differencing datasets where electrodes were replaced between data collections.

Table 1
Permanganate and RDX Concentrations from Direct-Push Sampling

Location[1]	Depth		$NaMnO_4$ Conc. (mg/L)	RDX Conc. (mg/L)
	Meters	Feet		
56-1	18.6–19.8	61–65	0	<5
	20.1–21.3	66–70	259	27
	21.6–22.9	71–75	0	<5
	23.2–24.4	76–80	0	n.a.
	24.7–25.9	81–85	0	195
	26.8–27.4	88–90	1797	176
72	23.2–24.4	76–80	0	24
	24.7–25.9	81–85	0	79
	26.8–27.4	88–90	148	145
	27.7–29.0	91–95	920	74
	29.6–30.5	97–100	0	13
	31.1–31.4	102–103	168	63
56-2	18.6–19.8	61–65	0	<5
	20.1–21.3	66–70	0	<5
	21.6–22.9	71–75	0	<5
	23.2–24.4	76–80	0	<5
	24.7–25.9	81–85	0	<5
	26.8–27.4	86–90	0	<5
	28.3–95.0	93–95	512	37

[1]Location corresponds to sampling points in Figure 1.

1.5 m, the fluids were moving in fingers that were below our resolution. While this does not eliminate the possibility of detecting the material, it limits the expected signal strength.

Electrical Resistivity-Permanganate Injectate Relationship

Following the injection, permanganate injectate samples were collected from the monitoring wells twice each week for 63 d. During this period, five to eight wells contained measurable quantities of permanganate. An analysis of the spatial and temporal relationship between ERI resistivity values and permanganate concentration was performed to determine if there was correlation between the two datasets. Although the data is limited due to the number of wells that captured permanganate movement (Albano et al. 2010), the relationship between ERI values, which are correlated as a proxy for hydraulic conductivity, was not related to the permanganate injectate concentration during the first 2 weeks after the injection. After that period, however, a weak relationship developed between the groundwater permanganate concentration and ERI measurements (Figure 8A). This relationship for the plume was stable from Day 14 to Day 45, with a logarithmic relationship (average $R^2 \approx 0.45$ during this period). During this time period, the slope and intercept values of this relationship remained stable (Figure 8B and 8C). Later, as the permanganate concentrations decreased, the relationship began to change. These limited data indicate that the

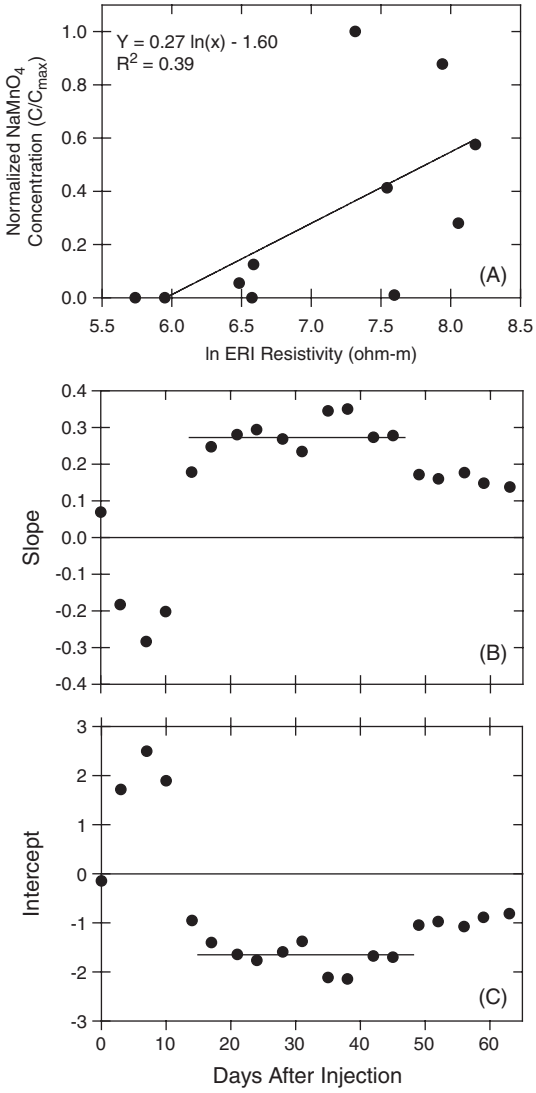

Figure 8. (A) Relationship between ERI resistivity data set (ln transformed) and normalized permanganate concentrations at 30 d postinjection. Change in slope (B) and intercept (C) of ERI-permanganate relationship for 63 d following injection.

ERI mapping allows a monitoring of the spatial distribution of permanganate as well as a mapping of the hydraulic conductivity distribution. Modifications to the monitoring protocol would be required to provide a direct mapping of concentration.

Lessons Learned for Mapping Injections with ERI

For future studies, modifications to the ERI monitoring approach and sampling protocols for the injection and well can improve results.

For ERI monitoring, three experimental procedures are suggested. First, semi-permanent electrodes should be installed at the surface for the duration of the experiment if possible. This was not possible at our site because part of the site was being actively farmed. Secondly, all ERI monitoring should be done assuming that transient data will be the only source of injectate monitoring data. Do not assume that even a strongly conductive fluid will be detected as a bulk resistivity change as fingering of injectate can provide a limited

amount of injectate in the image plane. Third, imaging for background fluid movement should be included at the same flow rates and locations as the planned injection prior to injection. This allows movement into the vadose zone to be characterized prior to using the injectate, and allows adjustment of the equipment to better image injectate.

For the injection, four factors should be kept in mind. First, assume that the injectate will primarily move up into the vadose zone. This was observed during this experiment and at two additional commercial sites using this technique (LLC Aestus, personal commication, 2009). If the material is to be delivered to the phreatic zone only, injection rates and monitoring should be adjusted to limit vertically upward movement of injectate. Secondly, any monitoring system should use smaller piezometers screen lengths to ensure less fluid mixing occurs in the samples for geophysical calibration. This is often difficult as injections are often performed on preexisting sites, but if shorter screens are an option, they should be installed based on the property distribution defined by ERI data, not simply on a regular grid. Third, injection curtains should be established at lower pumping rates to control fingering. The lower head changes in the aquifer will increase injection costs by increasing delivery times, but will likely improve delivery to the zones of interest. Finally, vertical gradients near injection zones need to be estimated to assist in predicting the movement of injectate. This would require additional coupled piezometers in the injection zone.

Conclusions

ERI corroborated an assessment of the heterogeneous hydraulic conductivity field observed in multilevel slug tests at the NOP site. This indicates that ERI or similar geophysical data (e.g., helicopter electromagnetic data) may be useful in aquifer characterization for sampling or planning remediation programs at the NOP site.

ERI was intended to be quantitatively compared with well samples as part of the analysis of the transient dataset. However, the injectate did not follow the preinjection horizontal hydraulic gradient, but the act of injecting altered the gradient such that the injectate did not flow to the majority of the wells. The data suggested that the injectate moved away from the wells approximately 15 m in preferred pathways in the vadose zone during the injection stage. An asymmetrical curtain of injectate formed upgradient from the injection/extraction well system observed in the well and ERI data. The injectate then appeared to have moved downward and beneath the monitoring wells. As the only time at which injectate was clearly detectable in the ERI pseudosections was immediately after injection, the signal included wetting of the vadose zone by the cone of injection, thus the signal was comprised of both injectate and changes in moisture content in the vadose zone.

ERI provided a useful noninvasive tool that assisted in analysis of a complex spatial and temporal distribution of injectate not matching monitoring well locations. Moreover, ERI provided a quantitative assessment of hydraulic conductivity and an ability to track the initial direction of injectate movement.

Acknowledgments

Funding was provided in part by the Environmental Security Technology Certification Program (ESTCP), project ER-0635 and EPA Region 7. Partial support was also provided by the University of Nebraska School of Natural Resources and Water Sciences Laboratory. We thank Tim Sickbert of Oklahoma State University for his assistance and Matt Marxsen of The University of Nebraska Conservation and Survey Division for drilling services and project support. This paper is a contribution of Agricultural Research Division Projects NEB-38-071. Dr Halihan has a managed conflict of interest with Oklahoma State University regarding the use of ERI developments.

References

Adam, M.L., S.D. Comfort, and D.D. Snow. 2004. Remediating RDX-contaminated ground water with permanganate: Laboratory investigations for the Pantex perched aquifer. *Journal Environmental Quality* 33, 2165–2173.

Albano, J.A. 2009. In situ chemical oxidation of RDX-contaminated ground water with permanganate at the Nebraska Ordnance plant. M.S. thesis, University of Nebraska-Lincoln, Lincoln, Nebraska.

Albano, J., S.D. Comfort, V. Zlotnik, T. Halihan, M. Burbach, C. Chokejaroenrat, S. Onanong, and W. Clayton. 2010. In situ chemical oxidation of RDX-contaminated ground water with permanganate at the Nebraska Ordnance Plant. *Ground Water Monitoring & Remediation* 30, no. 3: 96–106. DOI: 10.1111/j1745-6592.2010.01295.x.

Cavé, L., N. Hartog, T. Al, B. Parker, K.U. Mayer, and S. Cogswell. 2007. Electrical monitoring of in situ chemical oxidation by permanganate. *Ground Water Monitoring & Remediation* 27, no. 2: 77–84.

Chokejaroenrat, C., S.D. Comfort, C.E. Harris, D.D. Snow, D. Cassada, C. Sakulthaew, and T. Satapanajaru. 2011. Transformation of Hexahydro-1,3-5-trinitro-1,3,5-triazine (RDX) by permanganate. *Environmental Science & Technology* 45, no. 8: 3643–3649.

Comfort, S.D. 2005. Remediating RDX and HMX contaminated soil and water. In *Bioremediation of Aquatic and Terrestrial Ecosystems*, ed. M. Fingerton and R. Nagabhushanam, 263–310. Enfield, New Hampshire: Science Publishers.

Daily, W., A. Ramirez, A. Binley, and D. LaBrecque. 2004. Electrical resistance tomography. *Leading Edge* 23, no. 5: 438–442.

Halihan, T., S. Comfort, and V. Zlotnik. 2009. Using electrical resistivity imaging to evaluate permanganate performance during an in situ treatment of an RDX-contaminated aquifer. Environmental Security Technology Certification Program Final Report ER-0635. U.S. Department of Defense.

Halihan, T., and T. Fenstemaker. 2004. *Proprietary Electrical Resistivity Imaging Method*, 2nd ed. Stillwater, Oklahoma: Oklahoma State University Office of Intellectual Property.

Miall, A.D. 1977. A review of the braided-river depositional environment. *Earth-Science Reviews* 13, 1–62.

Nyquist, J.E., B.J. Carr, and R.K. Davis. 1999. DC resistivity monitoring of potassium permanganate injected to oxidize TCE in situ. *Journal of Environmental and Engineering Geophysics* 4, 135–147.

Ramirez, A., W. Daily, D. LaBrecque, E. Owen, and D. Chesnut. 1993. Monitoring an underground steam injection process using electrical resistance tomography. *Water Resources Research* 29, 73–87.

Seol, Y., H. Zhang, and F.W. Schwartz. 2003. A review of in situ chemical oxidation and heterogeneity. *Environmental and Engineering Geoscience* 9, no. 1: 37–49.

Singha, K., and S.M. Gorelick. 2006a. Hydrogeophysical tracking of 3D tracer migration: the concept and application of apparent petrophysical relations. *Water Resources Research* 42, W06422. DOI: 10.1029/2005WR004568.

Singha, K., and S.M. Gorelick. 2006b. *Effects of spatially variable resolution on field-scale estimates of tracer concentration from electrical inversions using Archie's law*. Geophysics 71, no. 3: G83–G91.

Telford, W.M., L.P. Geldart, and R.E. Sheriff. 1990. *Applied Geophysics,* 2nd ed., Cambridge: Cambridge University Press.

Wani, A.H., R. Wade, and J.L. Davis. 2007. Field demonstration of biologically active zone enhancement using acetate as a sole carbon source for in situ reductive transformation of RDX in groundwater. *Practical Periodical of Hazardous, Toxic, and Radioactive Waste Management* 11, no. 2: 83–91.

Woodward-Clyde. 1995. Engineering evaluation/cost analysis for operable unit No. 2 (groundwater) former Nebraska Ordnance Plant, Mead, Nebraska DACA 41-92-C-0023. Kansas City, Missouri: Department of the Army.

Zlotnik, V.A., and B.R. Zurbuchen. 2003. Field study of hydraulic conductivity in a heterogeneous aquifer: Comparison of single-borehole measurements using different instruments. *Water Resources. Research* 39, no. 4: 1101–1112. DOI: 10.1029/2002WR001415.

Zlotnik, V.A., and V.L. McGuire. 1998. Multi-level slug tests in highly permeable formations: 1. Modification of the Springer-Gelhar (SG) model. *Journal of Hydrology* 204, 271–282.

Zurbuchen, B.R., V.A. Zlotnik, and J.J. Butler. 2002. Dynamic interpretation of slug tests in highly permeable aquifers. *Water Resources Research* 38, no. 3: 1–18.

Biographical Sketches

***Todd Halihan**, corresponding author, is an associate professor of hydrogeology at the School of Geology, Oklahoma State University, Stillwater, OK 74078; (405) 744-9248; todd.halihan@okstate.edu.*

***Jeffrey Albano** has a masters of science in hydrogeology and is a hydrogeologist at CH2MHill, 11301 Carmel Commons Blvd. Suite 304, Charlotte, NC 28226.*

***Steve D. Comfort** is a professor of environmental chemistry at the School of Natural Resources, University of Nebraska, Lincoln, NE 68583-0915.*

***Vitaly A. Zlotnik** is a professor of hydrogeology at the Department of Earth and Atmospheric Sciences, University of Nebraska-Lincoln, Lincoln, NE 68588.*